



## **How do oncoming traffic and cyclist lane position influence cyclist overtaking by drivers?**

Downloaded from: <https://research.chalmers.se>, 2021-08-31 20:26 UTC

Citation for the original published paper (version of record):

Rasch, A., Åkerberg Boda, C., Thalya, P. et al (2020)

How do oncoming traffic and cyclist lane position influence cyclist overtaking by drivers?

Accident Analysis and Prevention, 142

<http://dx.doi.org/10.1016/j.aap.2020.105569>

N.B. When citing this work, cite the original published paper.



## How do oncoming traffic and cyclist lane position influence cyclist overtaking by drivers?



Alexander Rasch<sup>a,\*</sup>, Christian-Nils Boda<sup>a</sup>, Prateek Thalya<sup>a,b</sup>, Tobias Aderum<sup>b</sup>, Alessia Knauss<sup>b</sup>, Marco Dozza<sup>a</sup>

<sup>a</sup> Department of Mechanics and Maritime Sciences, Chalmers University of Technology, Hörselgången 4, 41756 Göteborg, Sweden

<sup>b</sup> Veoneer Research, Veoneer Sweden AB, Wallentinsvägen 22, 44737 Vårgårda, Sweden

### ARTICLE INFO

Editor: M.A. Abdel-Aty

#### Keywords:

Cycling safety  
Driver behaviour  
Driver assistance  
Test track  
Bayesian modelling

### ABSTRACT

Overtaking cyclists is challenging for drivers because it requires a well-timed, safe interaction between the driver, the cyclist, and the oncoming traffic. Previous research has investigated this manoeuvre in different experimental environments, including naturalistic driving, naturalistic cycling, and simulator studies. These studies highlight the significance of oncoming traffic—but did not extensively examine the influence of the cyclist's position within the lane.

In this study, we performed a test-track experiment to investigate how oncoming traffic and position of the cyclist within the lane influence overtaking. Participants overtook a robot cyclist, which was controlled to ride in two different lateral positions within the lane. At the same time, an oncoming robot vehicle was controlled to meet the participant's vehicle with either 6 or 9 s time-to-collision. The order of scenarios was randomised over participants. We analysed safety metrics for the four different overtaking phases, reflecting drivers' safety margins to rear-end, head-on, and side-swipe collisions, in order to investigate the two binary factors: 1) time gap between ego vehicle and oncoming vehicle, and 2) cyclist lateral position. Finally, the effects of these two factors on the safety metrics and the overtaking strategy (either *flying* or *accelerative* depending on whether the overtaking happened before or after the oncoming vehicle had passed) were analysed.

The results showed that, both when the cyclist rode closer to the centre of the lane and when the time gap to the oncoming vehicle was shorter, safety margins for all potential collisions decreased. Under these conditions, drivers—particularly female drivers—preferred accelerative over flying manoeuvres. Bayesian statistics modelled these results to inform the development of active safety systems that can support drivers in safely overtaking cyclists.

### 1. Introduction

Cycling is growing in popularity, due at least partly to its significant mobility and health benefits (de Hartog et al., 2010; Dozza et al., 2017; Pucher and Dijkstra, 2003) and the increasing market penetration of electric bicycles (Haustein and Møller, 2016; Wang et al., 2017). However, the risk of fatalities or severe injuries in crashes between cyclists and motorised vehicles is a big concern, especially on rural roads where dedicated cycle lanes are often absent and impact speeds are generally high (European Road Safety Observatory, 2018a; World Health Organization, 2018). The most common vehicle-to-cyclist crash scenario in crash databases involves a cyclist crossing in front of the vehicle; however, overtaking (or general longitudinal) scenarios

account for more severe injuries/fatalities, due to the high impact speed in rear-end collisions (Isaksson-Hellman and Werneke, 2017; Op den Camp et al., 2017). Poor timing during braking or steering away as a driver approaches a cyclist from behind can result in a rear-end collision (Kovaceva et al., 2019). Further, a too small lateral distance can cause the cyclist to lose balance and fall, due to aerodynamic pressure changes or even direct contact. Side-swipe collisions (Wood et al., 2009) can also occur if the driver steers back too early.

Active safety systems can assist the driver during overtaking (Hegeman et al., 2009), and help avoid rear-end crashes, for instance by applying autonomous emergency braking (AEB) or issuing forward collision warning (FCW) (European Road Safety Observatory, 2018b). In fact, since 2018, AEB and FCW systems have been rated by the

\* Corresponding author.

E-mail addresses: [alexander.rasch@chalmers.se](mailto:alexander.rasch@chalmers.se) (A. Rasch), [christian-nils.boda@chalmers.se](mailto:christian-nils.boda@chalmers.se) (C.-N. Boda), [prateek.thalya@veoneer.com](mailto:prateek.thalya@veoneer.com) (P. Thalya), [tobias.aderum@veoneer.com](mailto:tobias.aderum@veoneer.com) (T. Aderum), [alessia.knauss@veoneer.com](mailto:alessia.knauss@veoneer.com) (A. Knauss), [marco.dozza@chalmers.se](mailto:marco.dozza@chalmers.se) (M. Dozza).

<https://doi.org/10.1016/j.aap.2020.105569>

Received 29 November 2019; Received in revised form 14 April 2020; Accepted 18 April 2020

Available online 20 May 2020

0001-4575/ © 2020 The Authors. Published by Elsevier Ltd. This is an open access article under the CC BY-NC-ND license (<http://creativecommons.org/licenses/by-nc-nd/4.0/>).

European new car assessment program (Euro NCAP) for collision avoidance with cyclists, including scenarios for longitudinal collisions (Euro NCAP, 2019; Op den Camp et al., 2017). Ultimately, however, the systems' effectiveness depends on driver acceptance (Eichelberger and McCartt, 2016; Lubbe and Rosén, 2014). Brännström et al. (2013) proposed including driver behaviour models in active safety systems to ensure that early interventions/warnings would be accepted by drivers. Adapting to the framework of drivers' comfort zone (Ljung Aust and Engström, 2011), Ljung Aust and Dombrovski (2013) have suggested that the systems warn/intervene only when a driver has exceeded the comfort zone boundary. This study modelled drivers' comfort zone during overtaking to inform the design of active safety systems that can support drivers in safely overtaking cyclists.

Overtaking is a challenging task (Polus and Tomecki, 1987; Portouli et al., 2012), particularly since the driver's comfort zone is dependent on other road users (Gibson and Crooks, 1938). In the cyclist overtaking scenario, the cyclist and the oncoming traffic (when present) are the relevant road users. The lateral position of the cyclist within the lane has been identified as an important parameter (Op den Camp et al., 2017), although the extent to which this parameter influences the overall overtaking manoeuvre has not been studied in detail. Similarly, oncoming traffic is known to significantly influence driver behaviour, decreasing the vehicle's lateral distance from the cyclist (Bianchi Piccinini et al., 2018; Dozza et al., 2016; Kovaceva et al., 2019). However, the timing—in contrast to the mere presence or absence—of oncoming traffic has only been investigated in simulator studies by Bianchi Piccinini et al. (2018) and Farah et al. (2019). Those studies have shown that with shorter time gaps of the oncoming traffic, drivers tended to abort the overtaking attempt, or—if they overtook the cyclist anyway—left smaller safety margins to the cyclist (Bianchi Piccinini et al., 2018). Farah et al. (2019) used the same dataset to model the driver's decision whether to overtake or not, and the lateral comfort distance to the cyclist, with mixed-effect models. Nonetheless, simulator studies are known to have lower ecological validity than other environments like test tracks, especially in non-critical situations (Bianchi Piccinini et al., 2018; Farah et al., 2019), and do not preserve kinematic cues (Boda et al., 2018).

In this paper, we present a test-track study that investigated how 1) the cyclist's lane position and 2) the timing of the oncoming traffic influenced the risk of rear-end, head-on, and side-swipe collisions during an overtaking manoeuvre. The results from this study were modelled to offer a statistical description of driver comfort zone to be integrated in active safety systems.

## 2. Material and methods

### 2.1. Participants

Twenty-three employees from Autoliv and Veoneer were recruited as participants. There were two main criteria: 1) having a valid driver licence and 2) driving more than three times per week. The data from two participants were excluded from the analysis because of technical issues during the experiment. Three more participants were excluded because they reported that driving conditions did not feel natural. In particular, the three participants stated that the test-track environment did not feel realistic compared to a real road or that they felt stressed because they felt observed. Only the data and demographics from the remaining 18 participants are presented in this paper.

Before the experiment, all participants signed a consent form. The consent form and the protocol for this study were reviewed by the local ethical board in Göteborg, Sweden (Dn:600–17). The participants were 25–54 years old (average 42.9, standard deviation (SD) = 8.9), had held a driver's licence for 24.7 years on average (SD = 9.1), and drove an average annual mileage of 14,900 km (SD = 10,200). Participants (of whom 28 % were female) drove on average 12 times per week (SD = 6). All participants agreed to the usage of their data for analysis.

(a)



(b)



**Fig. 1.** The test-track experiment at Vårgårda airfield: The ego vehicle is approaching the cyclist dummy, mounted on a high-speed platform (panel a). Panel b shows the balloon vehicle used as an oncoming vehicle. A video of the trial is available: <https://youtu.be/AixQ189hMi4>.

### 2.2. Test-track setup

Data collection took place in April 2018 at the Vårgårda airfield, an outdoor test-track facility in Vårgårda, Sweden. A Volvo S60 (Fig. 1, panel a) with automatic transmission and a speed limiter was the ego vehicle driven by participants. A dummy cyclist mounted on a high-speed platform (HSP; Fig. 1, panel a) represented a cyclist travelling in a straight line. The HSP was accelerated at  $0.82 \text{ m/s}^2$  to 20 km/h. A balloon vehicle (Fig. 1, panel b) representing the oncoming vehicle was accelerated at  $1.00 \text{ m/s}^2$  to 40 km/h (its maximum speed). The HSP and the balloon vehicle were triggered when the ego vehicle passed a photocell; their trajectories were controlled through a communication server called CHRONOS (Bjelkeflo et al., 2018). High-precision real-time kinematic GPS data loggers were mounted on the ego vehicle, the HSP, and the oncoming vehicle. They recorded two-dimensional position data (within 0.02 m accuracy), speed (within 0.1 km/h accuracy) and heading angle (within  $0.1^\circ$  accuracy). Additionally, the controller area network (CAN) recorded the ego vehicle's steering wheel angle, brake and gas pedal states (in per cent: 100 % at full pedal depression), and turn indicator state (Boolean: on/off). Data from all three vehicles, sampled at 100 Hz, were synchronised in post-processing using the GPS reference time.

The participants overtook the cyclist in six separate trials, set up with variations of two independent variables: 1) time gap (between ego vehicle and oncoming vehicle) and 2) cyclist overlap as a measure of lateral position. Cyclist overlap is, per Euro NCAP testing conditions (Euro NCAP, 2019), defined as the ratio of the lateral position of the cyclist (with respect to the ego vehicle's line of travel) and the ego vehicle's width. Participants were instructed to keep the vehicle speed at 70 km/h, a speed that was compatible with the Euro NCAP test protocol. A speed limiter was activated at the beginning of each trial to keep the approaching speed as constant as possible; it was deactivated at 12 s time-to-collision (TTC) to the cyclist throughout all trials. The time gap variable was defined as the TTC to the oncoming vehicle when the ego vehicle reached a TTC of 2 s to the cyclist (Fig. 2). The intended time gap was either 6 s, 9 s, or none (oncoming vehicle absent). These

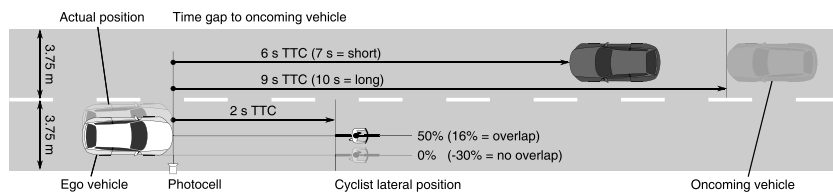


**Fig. 2.** The test-track setup included two levels of cyclist lateral position (planned values 0 %, 50 % overlap within vehicle width), and two different time gaps with the oncoming vehicle (6 s and 9 s time-to-collision, TTC), calculated from the position of the ego vehicle when the TTC to the rear of the cyclist was 2 s. The values in parentheses represent the actual measured values. The shaded ego vehicle marks the actual position by participants.

time gaps were chosen in accordance with Bianchi Piccinini et al. (2018). The intended overlap value, achieved by controlling the lateral position of the cyclist in the lane, was either 0 % or 50 %, according to the Euro NCAP test protocol (Euro NCAP, 2019). At the time when the experimental protocol was designed, 0 % overlap was still in the Euro NCAP test protocol, however, it has been replaced by 25 % (Euro NCAP, 2019). Permutation of the levels of the two variables resulted in six different trials, with the order randomised for each participant.

Before the experiment, each participant was given a description of the study and instructions by the test leader. After two test drives to get comfortable with the ego vehicle and the speed, the participants began the six trials. Participants were instructed to drive in the right lane and could overtake the cyclist if they wanted to. After each trial, the participants were asked to rate the discomfort felt while overtaking the cyclist: ‘On a scale from 1 to 7, where 1 is no discomfort and 7 is maximal discomfort, how did it feel to overtake the bike?’

Despite the plan to achieve a vehicle overlap of either 0 % or 50 %, the actual overlap values resulted in the medians -30 % and 16 %, referred to hereafter as *no overlap* and *overlap*, respectively (Fig. 2). This difference occurred because drivers did not stay in the middle of the lane as expected; instead, they positioned themselves on the left side of the lane (Fig. 2), probably because the cyclist influenced their safety margin, resulting in a field of safe travel (Gibson and Crooks, 1938) shifted toward the left side. Like the overlaps, the actual time gaps also differed from those planned. The recorded time gaps were centred around the medians 7 s and 10 s instead of the intended 6 s and 9 s, respectively. This difference may have been due to insufficient accuracy in the control of the oncoming vehicle or the drivers’ deviation from the instructed speed. We will refer to these recorded time gaps as *short* and *long*, respectively (Fig. 2). Four trials were removed from the analysis because the timing of the oncoming vehicle was disturbed by strong wind. Overall, 68 trials were analysed. When oncoming traffic was present drivers performed both flying (without speed reduction) and accelerative manoeuvres (reducing speed to let oncoming traffic pass before overtaking). Otherwise, drivers always performed flying manoeuvres. In this paper, we focused our analysis on trials with oncoming traffic to be able to 1) compare flying and accelerative manoeuvres and 2) determine the extent to which the time gap to oncoming traffic and the overlap with the cyclist influenced driver manoeuvring.

### 2.3. Classification of overtaking phases and strategies

In accordance with previous studies (Bianchi Piccinini et al., 2018; Dozza et al., 2016; Kovaceva et al., 2019), the overtaking manoeuvre was divided into four phases: 1) *approaching*, 2) *steering away*, 3) *passing*, and 4) *returning* (Fig. 3). The approaching phase started when the ego vehicle was 200 m away from the starting position of the cyclist.

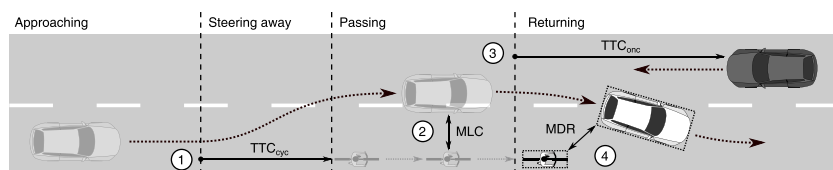


**Fig. 3.** Phases of a flying overtaking manoeuvre and related safety metrics: (1) Time-to-collision (TTC) to the cyclist at the beginning of the steering away phase, (2) Minimum lateral clearance (MLC) in the passing phase, (3) TTC to the oncoming vehicle, and (4) Minimum distance returning (MDR), measured as minimum Euclidean distance between the rectangular bounding boxes of ego vehicle and cyclist. An accelerative manoeuvre would look similar with the difference that the oncoming vehicle has already passed and that TTC to the cyclist is determined at brake onset.

The steering away phase started when the steering wheel angle last fell below -0.5 degrees (negative sign indicates anti-clockwise) before the steering wheel angle reached the negative peak amplitude of the final steering adjustment. The passing phase started when the lateral distance to the cyclist reached 0.2 m less than its maximum. The start of the returning phase was set to the last time that the lateral distance between the ego vehicle and the cyclist was 0.2 m smaller than its maximum. The end of the returning phase was set to the first time that the lateral distance was 0.2 m greater than its minimum.

The manoeuvre strategies were divided into *flying* (i.e. returning phase initiated before the oncoming vehicle passed or when the oncoming vehicle was absent) or *accelerative* (i.e. steering away phase initiated after decelerating to the cyclist’s speed and letting the oncoming vehicle pass). Accelerative manoeuvres are defined as such in the literature (Dozza et al., 2016; Feng et al., 2018; Matson and Forbes, 1938), because, after slowing down to the cyclist’s speed, the driver has to increase speed to perform the overtaking (which makes the manoeuvre differ from a simple following manoeuvre). For accelerative manoeuvres, the time of brake onset was set to the time after the start of the approaching phase when the brake pedal signal first exceeded 0.1 % deflection.

### 2.4. Safety metrics definitions

Four different crash risks were considered for the analysis, each addressing a different safety metric (see Fig. 3): 1) *rear-end* collision with the cyclist in the approaching phase, associated with the safety metric TTC<sub>cyc</sub> (TTC to the cyclist); 2) *side-swipe* collision with the cyclist in the passing phase; safety metric minimum lateral clearance (MLC); 3) *head-on* collision with the oncoming vehicle at the start of the returning phase (exists already in the passing phase but is highest at the end of it); safety metric TTC to the oncoming vehicle (TTC<sub>onc</sub>); and 4) *side-swipe* collision with the cyclist during the returning phase; safety metric minimum distance returning (MDR). Table 1 summarises the definitions of the safety metrics.

### 2.5. Bayesian regression models

We used Bayesian regression models to analyse the data and to draw quantitative conclusions (i.e., modelling safety metrics and determining the choice for overtaking strategy). Bayesian modelling is suitable because it can deal with different statistical distributions and estimate uncertainty in model parameters. In contrast to traditional frequentist methods, it provides access to the full posterior distribution of each parameter, contributing to the credibility of the results (Bürkner, 2017; Hoff et al., 2006; Kruschke, 2014).

Using the R Project’s software package *brms*, version 2.8.0 (Bürkner,

**Table 1**  
Summary of safety metrics, including the associated crash risk in the specific overtaking phase, as well as the definition.

Overtaking phase	Crash risk	Safety metric	Definition
Approaching	Rear-end collision with cyclist	TTC <sub>cyc</sub>	Time-to-collision (TTC) to cyclist at moment of action, i.e. at brake onset (accelerative manoeuvres) or at end of approaching phase (flying manoeuvres)
Passing	Side-swipe collision with cyclist while passing	MLC	Minimum lateral clearance during passing phase, measured as lateral distance between the bounding boxes of ego vehicle and cyclist
Passing	Head-on collision with oncoming vehicle (highest risk just before returning phase start)	TTC <sub>onc</sub>	TTC to the oncoming vehicle at the end of the passing phase (when the risk of head-on collision is highest)
Returning	Side-swipe collision with cyclist while returning	MDR	Minimum Euclidean distance between the bounding boxes of ego vehicle and cyclist during the returning phase

2017), Bayesian regression models with linear predictors were fitted to each of the safety metrics for each overtaking strategy as well as to the overtaking strategy choice itself. We chose log-normal distributions to model the safety metrics and a Bernoulli distribution to model the choice of strategy (flying or accelerative). Models were fitted with eight Markov chain Monte-Carlo (MCMC) chains, each containing 10,000 iterations. The first 5000 were used for warm-up by the MCMC algorithm and discarded after that. The number of iterations was chosen to be sufficiently large to guarantee convergence of the MCMC chains according to plots of their traces, and an *Rhat* value close to 1 (Bürkner, 2017). We used weakly informative default priors (Bürkner, 2018), following the practice of Williams et al. (2018). Models were initially set up to contain the cyclist lateral position/time gap interaction (referred to as *full* models). Driver identity (ID) was included as a group-level effect to account for inter-participant differences (Bürkner, 2017). *Simplified* models without the interaction were then compared to the full models using leave-one-out cross-validation (LOOCV)—or 10-fold cross-validation (where LOOCV failed), adapting the work of Vehtari et al. (2017). The best fit in terms of expected predictive accuracy was chosen. The differences between the model responses for the two levels of each factor (time gap or cyclist lateral position) were calculated using posterior predictive distributions. These differences, or contrasts, offer a way to determine the effect size and significance of a factor in a model: the 95 % highest-density interval (HDI) can be compared to a use-case-specific region of practical equivalence, typically centred around zero (Kruschke, 2018).

2.5.1. Model for overtaking strategy

The decision to perform a flying overtaking manoeuvre was modelled with a Bernoulli distribution. The response variable OT represents whether a manoeuvre strategy is flying (OT= 1) or accelerative (OT= 0). Since the dataset contained multiple events from same drivers, the driver identity (ID) was included as a group-level effect (Bürkner, 2018). The *i* th response of OT is modelled to be sampled from a Bernoulli distribution:

$$OT_i \sim \text{Bernoulli}(p_i), \tag{1}$$

where  $p_i$  is the predictor of the model, representing the probability that a random variable takes the value 1, i.e. the manoeuvre strategy is flying. The predictor is modelled by a linear combination of population- and group-level effects via a logit transformation:

$$\logit(p_i) = \log\left(\frac{p_i}{1 - p_i}\right) = \mathbf{X}_{OT,i} \boldsymbol{\beta} + \mathbf{Z}_{OT,ID,i} \mathbf{u}_{OT,ID},$$

$$\mathbf{u}_{OT,ID} \sim N(0, \sigma_{OT,ID}^2 \mathbf{I}), \tag{2}$$

where  $\boldsymbol{\beta}$  is the vector of population-level parameters and  $\mathbf{X}_{OT}$  the corresponding design matrix. The vector  $\boldsymbol{\beta}$  contains the parameters to be fitted, and is for the full model with the interaction defined as:

$$\boldsymbol{\beta} = [\beta_0 \ \beta_{clp} \ \beta_{tg} \ \beta_{clp*tg}]^T. \tag{3}$$

In Eq. (3),  $\beta_0$  is the intercept of the model,  $\beta_{clp}$  and  $\beta_{tg}$  are the parameters for the factors cyclist lateral position and time gap, respectively.

The \* operator marks the interaction between those factors. Each row *i* of the design matrix,  $\mathbf{X}_{OT,i}$  is accordingly defined as:

$$\mathbf{X}_{OT,i} = [1 \ X_{clp,i} \ X_{tg,i} \ X_{clp,i}X_{tg,i}], \tag{4}$$

where  $X_{clp,i}$  is the cyclist lateral position (0 = no overlap, 1 = overlap) and  $X_{tg,i}$  the time gap (0 = short, 1 = long).

In Eq. (2),  $\mathbf{Z}_{OT,ID,i}$  and  $\mathbf{u}_{OT,ID}$  represent the group-level effect of each driver (identity 'ID') on the intercept of the predictor.  $\mathbf{u}_{OT,ID}$  is sampled from a zero-centred, multivariate, normal distribution with covariance  $\sigma_{OT,ID}^2 \mathbf{I}$ .  $\mathbf{Z}_{OT,ID,i}$  is the *i* th row of the corresponding design matrix  $\mathbf{Z}_{OT,ID}$ .

2.5.2. Models for safety metrics

Let the safety metrics be summarised with SM:

$$SM = \{\text{TTC}_{cyc}, \text{MLC}, \text{TTC}_{onc}, \text{MDR}\}. \tag{5}$$

The safety metrics models were separated for flying and accelerative manoeuvres. For flying manoeuvres,  $\text{TTC}_{cyc}$  is the TTC at the beginning of the steering away phase, while for accelerative manoeuvres it is the TTC at brake onset. Since the oncoming vehicle had already passed for accelerative manoeuvres, the model for  $\text{TTC}_{onc}$  only exists for flying manoeuvres.

Since the safety metrics value distributions were positively skewed, a log-normal distribution was chosen to model each of the metrics. In Eq. (2), the model for the *i* th response variable  $SM_i$  is shown:

$$SM_i \sim \text{Lognormal}(\mu_{SM,i}, \sigma_{SM}). \tag{6}$$

where  $\mu_{SM,i}$  is the log-normal mean of the model, the (linear) predictor.  $\sigma_{SM}$  is the standard deviation of the log-normal distribution and assumed constant over all responses. The resulting predictor is:

$$\mu_{SM,i} = \mathbf{X}_{SM,i} \boldsymbol{\beta} + \mathbf{Z}_{SM,ID,i} \mathbf{u}_{SM,ID}, \ \mathbf{u}_{SM,ID} \sim N(0, \sigma_{SM,ID}^2 \mathbf{I}). \tag{7}$$

In Eq. (7),  $\boldsymbol{\beta}$  is the vector of population-level parameters, as defined in Eq. (4), and  $\mathbf{X}_{SM,i}$  is the corresponding design matrix.  $\mathbf{Z}_{SM,ID,i}$  and  $\mathbf{u}_{SM,ID}$  describe the group-level effect of the driver identity, as in Eq. (2).

3. Results

3.1. Overtaking strategy

Flying overtaking manoeuvres were more prevalent than accelerative manoeuvres overall (41 vs 27 observations overall; see Table 2), especially for long time gaps (31 vs 4). For short time gaps, accelerative manoeuvres were more common (23 vs 10). Female participants were more likely to perform accelerative manoeuvres than flying ones (11 vs 9) compared to male participants (16 vs 32). Higher discomfort was generally perceived 1) during accelerative overtaking compared to flying and 2) during flying overtaking with overlaps and short time gaps. Therefore, discomfort increased with criticality; however, this specific result was not further modelled in this study.

The lateral clearances indicate that drivers decided which manoeuvre strategy to follow when they were still far from the cyclist: Figure 4 (panels a and b) shows that the average clearance profiles for

**Table 2**

Number of trials (N) and gender distribution (female, f; male, m) for each type of scenario (i.e., cyclist lateral position no overlap vs overlap and time gap short vs long), the overtaking manoeuvres performed in each scenario (flying/accelerative), and the self-reported discomfort scores. Mean and standard deviation are reported for the discomfort scores.

	Cyclist lateral position	No overlap		Overlap	
		Short	Long	Short	Long
Gender distribution	Flying (N)	(1 f, 6 m)	(4 f, 13 m)	(0 f, 3 m)	(4 f, 10 m)
	Accelerative (N)	(4 f, 5 m)	(1 f, 0 m)	(5 f, 9 m)	(1 f, 2 m)
Discomfort score	Flying; mean (std)	2.4 (0.8)	2.1 (1.2)	3.7 (1.5)	2.2 (1.4)
	Accelerative; mean (std)	2.9 (1.8)	3.0 (0.0)	2.6 (1.6)	3.0 (1.0)

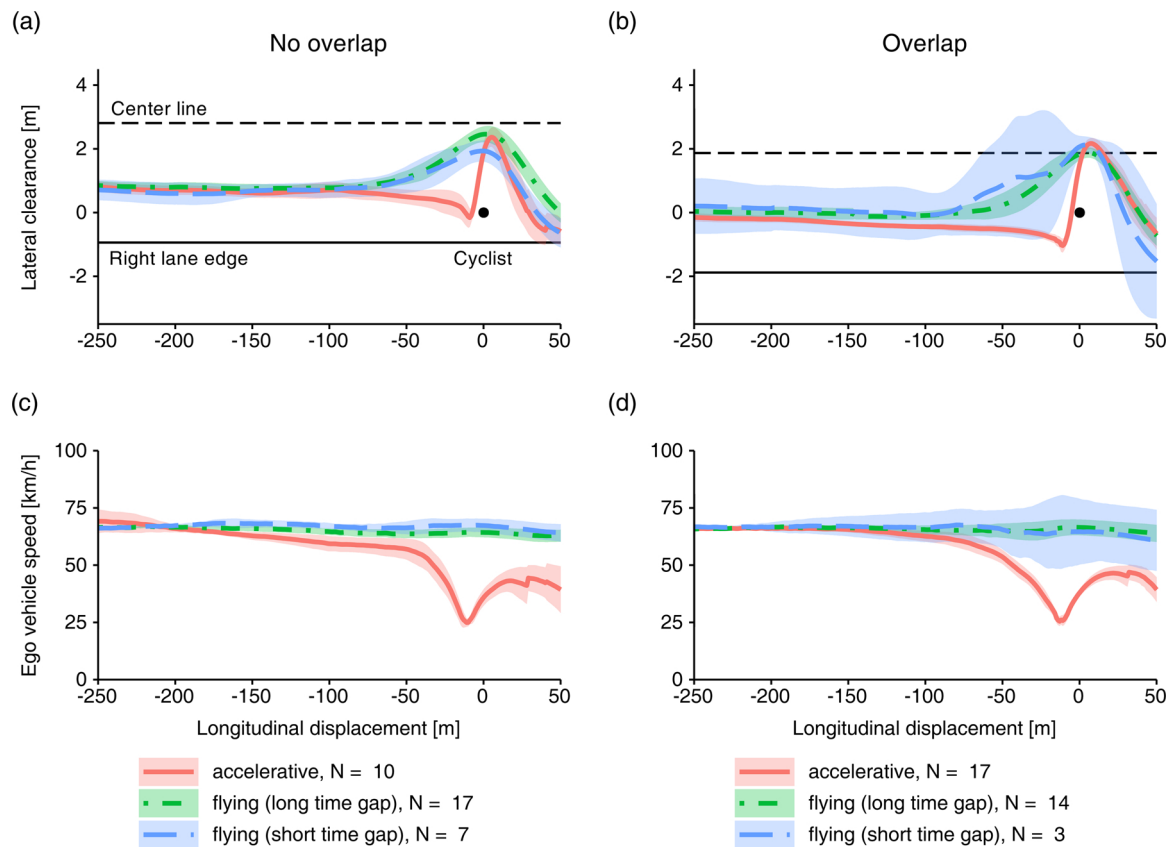


**Fig. 4.** Mean profiles (lines) and 95 % confidence intervals (shaded areas) over longitudinal displacement (distance from ego vehicle front bumper to cyclist rear wheel), grouped by manoeuvre strategy (flying/accelerative) and time gap (short/long). Small and large gaps are shown separately for flying manoeuvres; accelerative manoeuvres include both time gaps. Panels (a) and (b) show the lateral clearance between the cyclist and ego vehicle bounding boxes with no overlap and with overlap, respectively. Panels (c) and (d) show the ego vehicle speed with no overlap and with overlap, respectively.

flying and accelerative manoeuvres diverged when drivers were closer than 80 m from the cyclist. The speed profiles indicate that, with no overlap (panel c), the speed reduction was initiated later (120 m vs 200 m) than with overlap (panel d). With no overlap and the long time gap, drivers kept larger clearances when passing (panel a). In flying-manoeuvre trials with the overlap and the short time gap, the standard deviation of lateral clearance and speed is large, due perhaps to their rarity or to large behavioural differences across drivers. For accelerative manoeuvres, drivers tended to shift slightly back into their lane just before initiating the steering away phase; this behaviour is clearly visible in panels a and b.

The simplified Bayesian regression model for the strategy decision (i.e. without the interaction between cyclist lateral position and time gap) was equivalent (within standard error) to the full model in terms of predictive accuracy. The 10-fold cross-validation revealed that the

full model's expected log posterior density (Vehtari et al., 2017) was 10.76 higher than that of the simplified model; however, the standard error of this estimation was 10.18. Table 3 summarises the posterior distributions of the parameters of the simplified model, i.e. without the cyclist lateral position/time gap interaction, with the estimate (median) and the 95 % HDI. The full model is reported in Table A1 in Appendix A.

The contrasts in the (simplified) model response for the factors cyclist lateral position and time gap were estimated to be  $-0.12$  (median) with  $[-0.41, -0.03]$  95 % HDI and  $-0.88$  (median) with  $[-1.00, -0.55]$  95 % HDI, respectively. Contrasts from the data, estimated as the differences between the medians of each outcome of the factors, were  $-0.21$  and  $-0.58$  for overlap and time gap, respectively. These values lie within the 95 % HDI of the corresponding model responses, supporting the fit of the models.

**Table 3**

Overtaking strategy model parameter distributions, summarised with median and upper and lower bounds of highest-density interval (u-95 % HDI and l-95 % HDI, respectively), reported for the simplified model (without the interaction). The parameters of the predictor are denoted by  $\beta_0$  (intercept),  $\beta_{clp}$  (cyclist lateral position),  $\beta_{tg}$  (time gap) and  $\beta_{clp \times tg}$  (interaction between cyclist lateral position and time gap).  $\sigma_{OT,ID}$  is the standard deviation of the group-level effect of driver identity (ID).

Parameter	$\beta_0$	$\beta_{clp}$	$\beta_{tg}$	$\sigma_{OT,ID}$
Median	9.62	-3.62	-11.42	6.03
u-95 % HDI	18.74	-0.68	-3.18	12.43
l-95 % HDI	2.51	-7.04	-22.4	1.11

**3.2. Safety metrics**

All safety metrics generally decreased with overlap and short time gap (Fig. 5), except MDR, which increased with overlap (Fig. 5 panel d).

Table 4 reports the parameter estimates (medians) and 95 % HDIs of the simplified models, i.e. without the cyclist lateral position/time gap interaction. The LOOCV method confirmed that the simplified models were equivalent to (within standard error) or better fits than the full models (positive change in expected log posterior density, Table 4). The full models are reported in Table A2 in Appendix A.

Contrasts in the data, determined by the differences between the median values for each factor outcome, were within the 95 % HDI of the corresponding (simplified) models, supporting the fit of the models (Tab. 5). For flying manoeuvres, MLC was lower with overlap compared to no overlap: the whole 95 % HDI is below zero (with a similar trend for accelerative manoeuvres). Furthermore, for flying manoeuvres, the shorter the time gap, the more critical the MLC and  $TTC_{onc}$ . The 95 % HDIs of the contrasts for MDR and  $TTC_{cyc}$  contained neither fully

positive nor fully negative values and therefore did not indicate any significant results.

**4. Discussion**

**4.1. Driver behaviour**

Flying manoeuvres, in the presence of an overlap with the cyclist and a short time gap to the oncoming traffic, were the most critical and—according to the participants—uncomfortable. Understandably, the accelerative overtaking manoeuvre was preferred over the flying overtaking manoeuvre in those conditions. Female driver’s overtaking behaviour appeared to be more safety-conscious as they preferred accelerative manoeuvres even when male drivers still felt comfortable performing flying manoeuvres, as previously reported by Kovaceva et al. (2019). Other studies have shown that male drivers have a higher risk-taking propensity than female drivers (Harris et al., 2006). The Bayesian models revealed that time gap impacted strategy more than cyclist lateral position. The interaction with the oncoming vehicle is predominant from the passing phase onwards; the driver has to reconcile the risk for a head-on collision with the oncoming vehicle (greatest at the beginning of the returning phase) and a rear-end or side-swipe collision with the cyclist. In accelerative manoeuvres, the shift to the right within the lane that the overtaking vehicle makes before starting to overtake may be a signal to the oncoming traffic that the driver has seen it and will decelerate. Similar behaviour, observed in vehicle-to-vehicle overtaking manoeuvres, has been interpreted as communicating intent in the context of an interaction (Portouli et al., 2012). This behaviour may be important for the design of active safety systems and driver monitoring systems (Morando et al., 2020), because if the system can properly interpret the driver’s intent, it can provide timely accurate and acceptable warnings/interventions, as suggested by Morris et al. (2011). An alternative interpretation of the shift to the

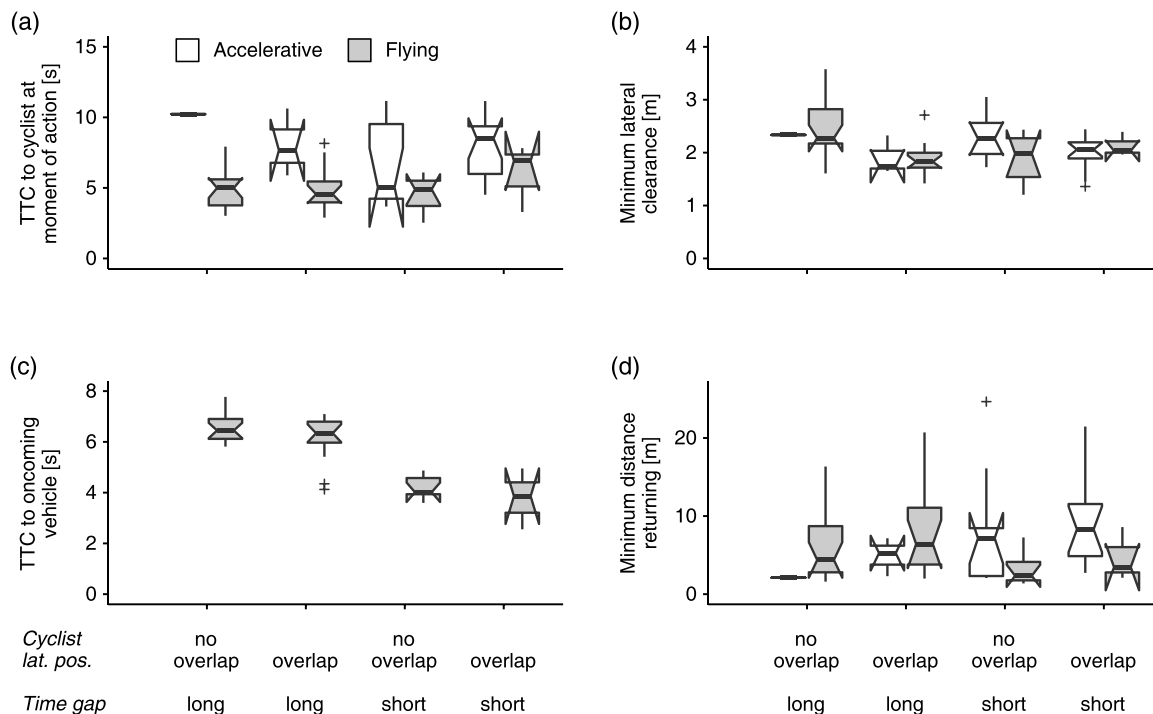


**Fig. 5.** Boxplot diagrams of safety metrics with respect to manoeuvre strategy (flying/accelerative) and factor (cyclist lateral position (lat. pos.)/time gap). Panel a): Time-to-collision (TTC) to cyclist, at steer away moment for flying and at brake onset for accelerative manoeuvres. Panel b): Minimum lateral clearance (MLC) in the passing phase. Panel c): TTC to oncoming vehicle at the end of the passing phase (flying manoeuvres only). Panel d): Minimum distance returning (MDR) in returning phase. The notches show the  $\pm 1.58/\sqrt{N}$  interquartile range (IQR) and the median (thick horizontal line) indicates the number of observations (N). The vertical lines indicate  $\pm 1.5$  IQR from the upper/lower hinges, and the ‘+’-signs represent outliers.

**Table 4**

Summary of estimated parameter values for each safety metric model. The medians and lower and upper limits of the 95 % highest-density intervals (HDI) are reported for the simplified model (without the interaction). Leave-one-out cross-validation reports the difference in expected log posterior density ( $\Delta$ ELPD), and the standard error (SE) in parentheses, for the comparison between the full and simplified models. A positive sign in  $\Delta$ ELPD indicates an improvement in predictive accuracy due to removing the interaction (included in the full model). The parameters of the predictor are denoted by  $\beta_0$  (intercept),  $\beta_{clip}$  (cyclist lateral position),  $\beta_{tg}$  (time gap), and  $\beta_{clip \cdot tg}$  (cyclist lateral position/time gap interaction).  $\sigma_{SM,ID}$  is the standard deviation of the group-level effect of driver identity (ID) on the predictor, and  $\sigma_{SM}$  is the standard deviation parameter of the log-normal distribution of the safety metric.

Strategy	Safety metric	$\Delta$ ELPD (SE)	Parameter	$\beta_0$	$\beta_{clip}$	$\beta_{tg}$	$\sigma_{SM,ID}$	$\sigma_{SM}$
Flying	TTC <sub>cyc</sub>	−0.85 (2.52)	Median	1.52	0.08	−0.01	0.15	0.27
			u-95 % HDI	1.67	0.26	0.20	0.27	0.35
			l-95 % HDI	1.37	−0.10	−0.22	0.00	0.20
	MLC	−1.43 (2.84)	Median	0.85	−0.19	−0.16	0.16	0.18
			u-95 % HDI	0.96	−0.07	−0.02	0.27	0.23
			l-95 % HDI	0.73	−0.31	−0.30	0.05	0.13
	TTC <sub>onc</sub>	3.56 (1.74)	Median	1.88	−0.09	−0.51	0.09	0.13
			u-95 % HDI	1.96	−0.01	−0.40	0.15	0.17
			l-95 % HDI	1.81	−0.17	−0.61	0.00	0.09
	MDR	−0.24 (2.15)	Median	1.63	0.19	−0.23	0.75	0.33
			u-95 % HDI	2.02	0.40	0.04	1.08	0.44
			l-95 % HDI	1.23	−0.05	−0.50	0.46	0.24
Accelerative	TTC <sub>cyc</sub>	8.08 (7.96)	Median	1.73	0.18	0.09	0.28	0.25
			u-95 % HDI	2.15	0.40	0.44	0.49	0.37
			l-95 % HDI	1.32	−0.04	−0.28	0.08	0.15
	MLC	9.68 (9.03)	Median	0.78	−0.11	0.00	0.15	0.12
			u-95 % HDI	0.97	0.00	0.16	0.27	0.19
			l-95 % HDI	0.59	−0.22	−0.16	0.02	0.07
	MDR	10.15 (8.87)	Median	1.30	0.33	0.42	0.63	0.46
			u-95 % HDI	2.02	0.76	1.03	1.08	0.72
			l-95 % HDI	0.54	−0.10	−0.20	0.20	0.25

right before overtaking is that the driver increases the lateral distance to the oncoming vehicle to increase her comfort zone and reduce the risk of a head-on collision (Gibson and Crooks, 1938).

The safety metrics were generally dependent on both factors (time gap and cyclist lateral position), and decreased as the criticality of the situation increased. The TTC<sub>cyc</sub> was not significantly influenced by either factor, suggesting that in the approaching phase the interaction between driver and cyclist has more influence on driver behaviour than the interaction between driver and oncoming traffic—possibly because at this point the driver’s main concern is to avoid a rear-end collision with the cyclist. The finding that MLC was lower with an overlap is in line with previous studies (Savolainen et al., 2013; Walker, 2007). Since an oncoming vehicle was present both with and without overlap, this finding can be explained as risk compensation because an oncoming vehicle is an additional risk to be handled by the driver (Wilde, 1982). With overlap, drivers reduce lateral clearance to the cyclist to reduce the risk of a head-on collision (which increases when they cross into the left lane). Note that drivers were not instructed to prefer the safety of one certain road user over the safety of the other. Analogously, the decrease in MLC consequent to the decreased time gap (for flying manoeuvres) may be explained by risk compensation: drivers compromise the safety margin to the cyclist with the increased head-on crash risk. This result also confirms previous findings from the simulator

study conducted by Bianchi Piccinini et al. (2018), who reported a decrease in lateral clearance with a reduced time gap to the oncoming traffic. The decrease in TTC<sub>onc</sub> (about 2 s) with a decrease in time gap at the start of the return phase suggests that the actual time gaps were able to capture a change in driver behaviour associated with the risk of a head-on collision. MDR was found to be lowest in the short-time-gap trials but largest in the overlap trials; drivers might be more aware of cyclists who are farther into their lane, and thus might return to the lane more carefully.

4.2. Active safety

A high percentile of the HDI of the predicted response from a Bayesian model (e.g. 95 %) can serve as a reference for active safety systems (Morando et al., 2020), quantifying drivers’ comfort zone during overtaking. Once the measured value of a safety metric during driving lies outside of the 95 % HDI (specifically below the lower bound of the interval), we assume that the driver has exceeded the comfort zone and a warning or intervention from the system may, therefore, be acceptable. The derived posterior distributions of the model parameters from the Bayesian model can become prior distributions for future studies and can also be incorporated as driver comfort into the systems’ threat assessment. A model capable of dynamic updates for individual

**Table 5**

Contrasts from posterior prediction of safety metrics models, including the differences between the medians for each condition in the data (labelled Data), the median differences from the model predictions (labelled Median), and the lower and upper 95 % highest-density intervals (l-95 % HDI and u-95 % HDI, respectively).

Strategy	Safety metric	Cyclist lateral position (overlap – no overlap)				Time gap (short – long)			
		Data	Median	l-95 % HDI	u-95 % HDI	Data	Median	l-95 % HDI	u-95 % HDI
Flying	TTC <sub>cyc</sub> [s]	−0.26	0.42	−0.82	1.66	0.32	−0.15	−1.51	1.29
	MLC [m]	−0.37	−0.36	−0.69	−0.02	−0.09	−0.28	−0.65	0.11
	TTC <sub>onc</sub> [s]	−0.21	−0.22	−0.89	0.46	−2.46	−2.49	−3.10	−1.81
	MDR [m]	2.39	1.15	−0.58	3.30	−2.94	−1.31	−3.38	0.56
Accelerative	TTC <sub>cyc</sub> [s]	3.28	1.17	−1.00	3.26	−2.78	0.56	−3.03	3.34
	MLC [m]	−0.25	−0.22	−0.57	0.08	0.08	0.04	−0.40	0.46
	MDR [m]	0.15	2.11	−2.29	7.01	3.62	2.42	−3.17	7.56



drivers (for instance, after an overtaking manoeuvre) could further improve active safety. A model that can determine which overtaking strategy (accelerative/flying) a driver will prefer might enable the safety system to predict the likelihood that the driver will abort an overtaking manoeuvre (accelerative instead of flying), as proposed by Farah et al. (2019). If the model shows that the manoeuvre is likely to be aborted, but the driver does not abort, FCW and AEB systems (or a pre-brake system) may assist the driver, avoiding a rear-end collision with the cyclist.

The Euro NCAP test protocol (longitudinal collision scenario with 25 % overlap) specifies an activation threshold for FCW of 1.7 s TTC<sub>cyc</sub> in order to award any rating points (Euro NCAP, 2019). The participants in our study would probably have accepted this threshold, because the median values for TTC for steering away/brake onset were well above 1.7 s: mean TTC<sub>cyc</sub> was 7.52 s (SD = 2.50, min = 3.68) for accelerative and 4.92 s (SD = 1.44, min = 2.53) for flying manoeuvres.

The Bayesian models from this study may support automated driving features by providing reference values for comfortable manoeuvres. However, it should be noted that automated vehicles might need to manoeuvre more conservatively compared to humans to be accepted (Abe et al., 2018; Farah et al., 2019). To meet this need, our models could be scaled to the most conservative human drivers within the data sample. This practice would be a better alternative than simply reducing safety margins threshold.

#### 4.3. Limitations and future work

The data in this study were collected on an airfield test track, where a straight-road overtaking scenario was created with robots and precisely repeated for each participant. Participants were recruited from two companies which produce safety systems; however, the participants were not involved in system development or design. On the contrary, they came from the finance and production department to minimise possible biases. The test-track setup is therefore limited in a way that naturalistic driving studies are not; nevertheless, test-track data still provide higher ecological validity than previous overtaking studies based on simulator data. The use of a dummy cyclist ignores the possible impact of cyclist appearance on overall driver behaviour, an effect reported by Lahrmann et al. (2018) and Walker (2007). However, the dummy's appearance from behind was very similar to a human rider on a real bicycle with legs moving and remained the same across the entire experiment—so there was no reason to believe that the trends across conditions were based on the cyclist's appearance alone. The oncoming balloon vehicle may have lacked realism as some participants noted that it did not have the headlights on (which is a legal requirement on Swedish rural roads). Some participant also mentioned that it was difficult to know if the vehicle was moving or stationary. However, our results show that participants still interacted with the oncoming vehicle (representing a threat to them), in a similar way as previously observed in naturalistic studies.

As a further limitation, the discomfort scores should be interpreted with caution, as the scale of discomfort used in this study has not yet been validated.

Future research should also investigate cyclist comfort, to compare the cyclist's comfort zone with that of the driver during an overtaking manoeuvre. For instance, in a naturalistic cycling study, the cyclist could flag whether an overtaking felt comfortable or not. This information could lead to 'fair' safety systems that maximise safety for all road users, while considering both driver and cyclist acceptance. Due to the limited sample size and to allow a descriptive analysis of the overtaking manoeuvre, the analyses considered the factors time gap and cyclist lateral position as binary. However, because these are both actually continuous measures, future studies should collect larger datasets or explore other modelling approaches to treat these factors as

continuous. A time-series prediction of driver behaviour during overtaking, including driver input actions such as braking, accelerating and steering, should also be developed. Safety systems incorporating more comprehensive models of driver-cyclist interactions could better support the driver and further reduce crash risk during overtaking. The models could also enable automated vehicles to behave more like human-driven vehicles.

## 5. Conclusions

Our results show that drivers' strategy in overtaking manoeuvres (flying or accelerative) is related to gender, the time gap between the ego and the oncoming vehicle, and the lateral position of the cyclist during the approach. The time gap to the oncoming vehicle was found to influence the strategy choice to a larger extent than the cyclist's lateral position. Safety metrics during the entire manoeuvre decreased when the time gap was short, or the cyclist rode farther left in the lane; this was not surprising, as cyclist safety is most endangered under these conditions. Drivers appeared to compromise head-on crash risk (with the oncoming traffic) with side-swipe crash risk (with the cyclist), illustrating the need for active safety systems which can support the driver before and during the *whole* overtaking manoeuvre. The models presented in this paper can be used to further develop driver monitoring systems and improve acceptance of active safety systems interventions to ensure safe and comfortable overtaking manoeuvres.

#### CRedit authorship contribution statement

**Alexander Rasch:** Software, Validation, Formal analysis, Data curation, Writing - original draft, Writing - review & editing, Visualization. **Christian-Nils Boda:** Conceptualization, Methodology, Software, Formal analysis, Investigation, Data curation, Writing - review & editing. **Prateek Thalya:** Methodology, Investigation, Writing - review & editing. **Tobias Aderum:** Resources, Writing - review & editing, Project administration. **Alessia Knauss:** Investigation, Resources, Writing - review & editing, Supervision, Project administration. **Marco Dozza:** Conceptualization, Methodology, Writing - review & editing, Supervision, Project administration, Funding acquisition.

#### Declaration of Competing Interest

The authors declare that they have no known competing financial interests or personal relationships that could have appeared to influence the work reported in this paper.

#### Acknowledgements

The authors would like to thank Nils Lubbe, Rustem Elezovic, Sebastian Kruger, Johan Holmsten, Daniel Nylen, John Lang, and Markus Pastuhoff for the support in conducting the test-track experiment. We thank Kristina Mayberry for language revisions of the manuscript.

This study was part of the project *Modelling Interaction between Cyclists and Automobiles*, funded jointly by Vinnova (Sweden), the Swedish Energy Agency (Sweden), the Swedish Transport Administration (Sweden), and the Swedish vehicle industry (Sweden) through the strategic vehicle research and innovation (FFI) program. The data collection and analysis were carried out in collaboration with the project *Drivers in Interaction with Vulnerable Road Users*, funded by Toyota Motor Europe (Belgium), Autoliv (Sweden) and Veoneer (Sweden). The work was carried out at the *SAFER Vehicle and Traffic Safety Centre at Chalmers*, Göteborg, Sweden.

Appendix A

Table A1

Overtaking strategy model parameter distributions, summarised with median and upper and lower bounds of highest-density interval (u-95 % HDI and l-95 % HDI, respectively). Reported is the full model, i.e. including the interaction between cyclist lateral position and time gap. The parameters of the predictor are denoted by  $\beta_0$  (intercept),  $\beta_{clp}$  (cyclist lateral position),  $\beta_{tg}$  (time gap) and  $\beta_{clp*tg}$  (interaction between cyclist lateral position and time gap).  $\sigma_{OT,ID}$  is the standard deviation of the group-level effect of driver identity (ID).

Parameter	$\beta_0$	$\beta_{clp}$	$\beta_{tg}$	$\beta_{clp*tg}$	$\sigma_{OT,ID}$
Median	14.24	-7.22	-17.25	3.39	8.07
u-95 % HDI	31.26	1.09	-2.77	15.5	17.77
l-95 % HDI	2.14	-19.69	-38.9	-5.78	1.44

Table A2

Summary of estimated parameter values for each safety metric model. Reported are the full models, i.e. including the interaction between cyclist lateral position and time gap. The medians and lower and upper limits of the 95 % highest-density intervals (HDI) are reported. The parameters of the predictor are denoted by  $\beta_0$  (intercept),  $\beta_{clp}$  (cyclist lateral position),  $\beta_{tg}$  (time gap), and  $\beta_{clp*tg}$  (cyclist lateral position/time gap interaction).  $\sigma_{SM,ID}$  is the standard deviation of the group-level effect of driver identity (ID) on the predictor, and  $\sigma_{SM}$  is the standard deviation parameter of the log-normal distribution of the safety metric.

Strategy	Safety metric	Parameter	$\beta_0$	$\beta_{clp}$	$\beta_{tg}$	$\beta_{clp*tg}$	$\sigma_{SM,ID}$	$\sigma_{SM}$
Flying	TTC <sub>cyc</sub>	Median	1.55	0.02	-0.14	0.35	0.18	0.25
		u-95 % HDI	1.70	0.20	0.11	0.77	0.32	0.33
		l-95 % HDI	1.39	-0.16	-0.38	-0.06	0.02	0.18
	MLC	Median	0.87	-0.25	-0.26	0.31	0.15	0.17
		u-95 % HDI	0.98	-0.13	-0.10	0.60	0.26	0.22
		l-95 % HDI	0.76	-0.38	-0.42	0.03	0.04	0.12
	TTC <sub>onc</sub>	Median	1.88	-0.09	-0.50	-0.01	0.08	0.13
		u-95 % HDI	1.96	0.01	-0.37	0.20	0.15	0.17
		l-95 % HDI	1.81	-0.18	-0.63	-0.23	0.00	0.09
	MDR	Median	1.60	0.26	-0.10	-0.39	0.77	0.31
		u-95 % HDI	2.00	0.50	0.21	0.15	1.10	0.42
		l-95 % HDI	1.19	0.04	-0.41	-0.92	0.48	0.22
Accelerative	TTC <sub>cyc</sub>	Median	1.98	-0.13	-0.18	0.35	0.26	0.26
		u-95 % HDI	2.64	0.49	0.43	1.03	0.47	0.39
		l-95 % HDI	1.37	-0.78	-0.85	-0.32	0.05	0.15
	MLC	Median	0.88	-0.23	-0.10	0.14	0.15	0.12
		u-95 % HDI	1.17	0.09	0.20	0.47	0.27	0.19
		l-95 % HDI	0.59	-0.53	-0.38	-0.19	0.02	0.06
	MDR	Median	1.14	0.51	0.60	-0.22	0.59	0.50
		u-95 % HDI	2.31	1.81	1.82	1.10	1.04	0.79
		l-95 % HDI	-0.10	-0.73	-0.62	-1.60	0.11	0.27

References

Abe, G., Sato, K., Itoh, M., 2018. Driver trust in automated driving systems: the case of overtaking and passing. *IEEE Trans. Human-Machine Syst.* 48 (1), 85–94. <https://doi.org/10.1109/THMS.2017.2781619>.

Bianchi Piccinini, G.F., Moretto, C., Zhou, H., Itoh, M., 2018. Influence of oncoming traffic on drivers' overtaking of cyclists. *Transp. Res. Part F Traffic Psychol. Behav.* 59, 378–388. <https://doi.org/10.1016/j.trf.2018.09.009>.

Bjelkefjo, L., Laxing, R., Djup, M., Gustafsson, P., Lundin, N., Johansson, V., Naterjee, V., Pohl, J., Schiller, E., Svensson, B.J., 2018. CHRONOS Part 1. Accessed November 27, 2019. <https://www.vinnova.se/globalassets/mikrosajter/ffi/dokument/slutrapporter-ffi/elektronik-mjukvara-och-kommunikation-rapporter/2016-02573.pdf>.

Boda, C.N., Dozza, M., Bohman, K., Thalya, P., Larsson, A., Lubbe, N., 2018. Modelling how drivers respond to a bicyclist crossing their path at an intersection: how do test track and driving simulator compare? *Accid. Anal. Prev.* 111 (October 2017), 238–250. <https://doi.org/10.1016/j.aap.2017.11.032>.

Brännström, M., Sandblom, F., Hammarstrand, L., 2013. A probabilistic framework for decision-making in collision avoidance systems. *IEEE trans. Intell. Transp. Syst.* 14 (2), 637–648. <https://doi.org/10.1109/TITS.2012.2227474>.

Bürkner, P.-C., 2017. Brms: an r package for bayesian multilevel models using stan. *J. Stat. Softw.* 80 (1). <https://doi.org/10.18637/jss.v080.i01>.

Bürkner, P.-C., 2018. Package "brms". <https://doi.org/10.18637/jss.v080.i01>.

de Hartog, J.J., Boogaard, H., Nijland, H., Hoek, G., 2010. Do the health benefits of cycling outweigh the risks? *Environ. Health Perspect.* 118 (8), 1109–1116. <https://doi.org/10.1289/ehp.0901747>.

Dozza, M., Schindler, R., Bianchi-Piccinini, G., Karlsson, J., 2016. How do drivers overtake cyclists? *Accid. Anal. Prev.* 88 (March (2016)). <https://doi.org/10.1016/j.aap.2015.12.008>.

Dozza, M., Schwab, A., Wegman, F., 2017. Safety science special issue on cycling safety. *Saf. Sci.* 92, 262–263. <https://doi.org/10.1016/j.ssci.2016.06.009>.

Eichelberger, A.H., McCart, A.T., 2016. Toyota drivers' experiences with dynamic radar cruise control, pre-collision system, and lane-keeping assist. *J. Safety Res.* 56, 67–73. <https://doi.org/10.1016/j.jsr.2015.12.002>.

Euro NCAP, 2019. Test Protocol - AEB VRU Systems. Accessed November 27, 2019. <https://cdn.euroncap.com/media/43381/euro-ncap-aeb-vru-test-protocol-v204.pdf>.

European Road Safety Observatory, 2018a. Pedestrians and Cyclists. Accessed November 27, 2019. [https://ec.europa.eu/transport/road\\_safety/sites/roadsafety/files/pdf/ersosynthesis2018-pedestrianscyclists.pdf](https://ec.europa.eu/transport/road_safety/sites/roadsafety/files/pdf/ersosynthesis2018-pedestrianscyclists.pdf).

European Road Safety Observatory, 2018b. Advanced Driver Assistance Systems. Accessed November 27, 2019. [https://ec.europa.eu/transport/road\\_safety/sites/roadsafety/files/pdf/ersosynthesis2018-adass.pdf](https://ec.europa.eu/transport/road_safety/sites/roadsafety/files/pdf/ersosynthesis2018-adass.pdf).

Farah, H., Bianchi Piccinini, G., Itoh, M., Dozza, M., 2019. Modelling overtaking strategy and lateral distance in car-to-cyclist overtaking on rural roads: a driving simulator experiment. *Transp. Res. Part F Traffic Psychol. Behav.* 63, 226–239. <https://doi.org/10.1016/j.trf.2019.04.026>.

Feng, F., Bao, S., Hampshire, R.C., Delp, M., 2018. Drivers overtaking bicyclists—an examination using naturalistic driving data. *Accid. Anal. Prev.* 115 (November 2017), 98–109. <https://doi.org/10.1016/j.aap.2018.03.010>.

Gibson, J.J., Crooks, L.E., 1938. A theoretical field-analysis of automobile-driving. *Am. J. Psychol.* 51 (3), 453–471.

Harris, C.R., Jenkins, M., Glaser, D., 2006. Gender differences in risk assessment: why do women take fewer risks than men? *Judgm. Decis. Mak.* 1 (1), 48–63.

Haustein, S., Möller, M., 2016. E-bike safety: individual-level factors and incident characteristics. *J. Transp. Heal.* 3 (3), 386–394. <https://doi.org/10.1016/J.JTH.2016.07.001>.

Hegeman, G., Tapani, A., Hoogendoorn, S., 2009. Overtaking assistant assessment using traffic simulation. *Transp. Res. Part C Emerg. Technol.* 17 (6), 617–630. <https://doi.org/10.1016/j.trc.2009.04.010>.

- Hoff, P., Casella, G., Fienberg, S., Olkin, I., 2006. A First Course in Bayesian Statistics. Springer <https://doi.org/10.1016/j.peva.2007.06.006>.
- Isaksson-Hellman, I., Werneke, J., 2017. Detailed description of bicycle and passenger car collisions based on insurance claims. *Saf. Sci.* 92, 330–337. <https://doi.org/10.1016/J.SSCI.2016.02.008>.
- Kovaceva, J., Nero, G., Bärngman, J., Dozza, M., 2019. Drivers overtaking cyclists in the real-world: evidence from a naturalistic driving study. *Saf. Sci.* 119 (Nov. (2019)), 119–206. <https://doi.org/10.1016/j.ssci.2018.08.022>.
- Kruschke, J.K., 2014. Doing bayesian data analysis: a tutorial with R, JAGS, and stan, second edition. *Doing Bayesian Data Analysis: a Tutorial With R, JAGS, and Stan*, second edition. <https://doi.org/10.1016/B978-0-12-405888-0.09999-2>.
- Kruschke, J.K., 2018. Rejecting or accepting parameter values in bayesian estimation. *Adv. Methods Pract. Psychol. Sci.* 1 (2), 270–280. <https://doi.org/10.1177/2515245918771304>.
- Lahrman, H., Madsen, T.K.O., Olesen, A.V., Madsen, J.C.O., Hels, T., 2018. The effect of a yellow bicycle jacket on cyclist accidents. *Saf. Sci.* 108 (August 2017), 209–217. <https://doi.org/10.1016/j.ssci.2017.08.001>.
- Ljung Aust, M., Dombrowski, S., 2013. Understanding and improving driver compliance with safety system. in: *The 23th International Technical Conference on the Enhanced Safety of Vehicles (ESV)*.
- Ljung Aust, M., Engström, J., 2011. A conceptual framework for requirement specification and evaluation of active safety functions. *Theor. Issues Ergon. Sci.* 12 (1), 44–65. <https://doi.org/10.1080/14639220903470213>.
- Lubbe, N., Rosén, E., 2014. Pedestrian crossing situations: quantification of comfort boundaries to guide intervention timing. *Accid. Anal. Prev.* 71, 261–266. <https://doi.org/10.1016/J.AAP.2014.05.029>.
- Matson, T.M., Forbes, T., 1938. Overtaking and passing requirements as determined from a moving vehicle. *Highw. Res. Board Proc.* 18, 100–112.
- Morando, A., Victor, T., Dozza, M., 2020. A bayesian reference driving model for visual time-sharing behaviour in manual and automated naturalistic driving. *IEEE trans. Intell. Transp. Syst.* 21 (2), 803–814. <https://doi.org/10.1109/TITS.2019.2900436>.
- Morris, B., Doshi, A., Trivedi, M., 2011. Lane change intent prediction for driver assistance: on-road design and evaluation. *IEEE Intell. Veh. Symp. Proc.* Iv 895–901. <https://doi.org/10.1109/IVS.2011.5940538>.
- Op den Camp, O., van Montfort, S., Uittenbogaard, J., Welten, J., 2017. Cyclist target and test setup for evaluation of cyclist-autonomous emergency braking. *Int. J. Automot. Technol. Manag.* 18 (6), 1085–1097. <https://doi.org/10.1007/s12239-017-0106-5>.
- Polus, A., Tomecki, A.B., 1987. Passing experiment on two-lane rural highways. *Transp. Res. Rec.* 1112, 115–123.
- Portouli, E., Nathanael, D., Marmaras, N., Papakostopoulos, V., 2012. Naturalistic observation of drivers' interactions while overtaking on an undivided road. in: *Work*. 4185–4191. <https://doi.org/10.3233/WOR-2012-0120-4185>.
- Pucher, J., Dijkstra, L., 2003. Promoting safe walking and cycling to improve public health: lessons from the Netherlands and Germany. *Am. J. Public Health* 93 (9), 1509–1516. <https://doi.org/10.2105/AJPH.93.9.1509>.
- Savolainen, P.T., Gates, T.J., Todd, R.G., Datta, T.K., Morena, J.G., 2013. Lateral placement of motor vehicles when passing bicyclists. *Transp. Res. Rec. J. Transp. Res. Board* 2314 (1), 14–21. <https://doi.org/10.3141/2314-03>.
- Vehtari, A., Gelman, A., Gabry, J., 2017. Practical Bayesian model evaluation using leave-one-out cross-validation and WAIC. *Stat. Comput.* 27 (5), 1413–1432. <https://doi.org/10.1007/s11222-016-9696-4>.
- Walker, I., 2007. Drivers overtaking bicyclists: objective data on the effects of riding position, helmet use, vehicle type and apparent gender. *Accid. Anal. Prev.* 39 (2), 417–425. <https://doi.org/10.1016/j.aap.2006.08.010>.
- Wang, C., Xu, C., Xia, J., Qian, Z., 2017. Modeling faults among e-bike-related fatal crashes in China. *Traffic Inj. Prev.* 18 (2), 175–181. <https://doi.org/10.1080/15389588.2016.1228922>.
- Wilde, G.J.S., 1982. The theory of risk homeostasis: implications for safety and health. *Risk Anal.* 2 (4), 209–225. <https://doi.org/10.1111/j.1539-6924.1982.tb01384.x>.
- Williams, D.R., Rast, P., Bürkner, P.-C., 2018. Bayesian meta-analysis with weakly informative prior distributions. *PsyArXiv* 1–19. <https://doi.org/10.31234/osf.io/7tbrm>.
- Wood, J.M., Lacherez, P.F., Marszalek, R.P., King, M.J., 2009. Drivers' and cyclists' experiences of sharing the road: incidents, attitudes and perceptions of visibility. *Accid. Anal. Prev.* 41 (4), 772–776. <https://doi.org/10.1016/j.aap.2009.03.014>.
- World Health Organization, 2018. *Global Status Report on Road Safety*. Accessed November 27, 2019. <https://apps.who.int/iris/bitstream/handle/10665/276462/9789241565684-eng.pdf?ua=1>.